Sādhanā (2022)47:266
https://doi.org/10.1007/s12046-022-02028-5

Biomechanical analysis head–neck injuries against mine falls using a simplified human model

RACHIT GARG[1], LINXIA GU[2] and SHAILESH GANPULE[1,3,*]

[1]Department of Mechanical and Industrial Engineering, Indian Institute of Technology Roorkee, Roorkee, Uttarakhand 247667, India
[2]Department of Biomedical and Chemical Engineering, Florida Tech University, Melbourne, FL 32901, USA
[3]Department of Design, Indian Institute of Technology Roorkee, Roorkee, Uttarakhand 247667, India
e-mail: rgarg1@me.iitr.ac.in; gul@fit.edu; ganpule@me.iitr.ac.in

MS received 12 April 2022; revised 28 July 2022; accepted 23 September 2022

Abstract. Fall-related mine fatalities remain one of the most critical threats to the miner's safety. Recent statistics suggest significant severe injuries from ground falls during mining operations, with head and neck being typically injured organs. The effectiveness of the existing miner's helmet in protection against ground falls is not known. In this work, we investigate the biomechanical response of the head and neck against the roof falls with and without the helmet. Towards this end, a simplified human finite element model is built. The model response is compared against the relevant experimental data, and the agreement between experiment and model predictions is reasonable. The model is subjected to roof fall with roof velocities of 1, 3, and 6 m/s, and the biomechanical response of the brain and neck is studied. Various helmet configurations consisting of hard and soft layers have been investigated. Our results suggest that existing helmets reduce the strains and stresses in the brain by upto ∼59%. On the contrary, the neck forces and moments have increased with helmets by upto ∼86%. This is due to the increase in mass of the system due to the addition of the helmet. We also observe that even though stresses in the brain have been reduced with the helmet, the reduction offered by the helmet may not be sufficient to prevent mild TBI. Overall, our results suggest that the role of the miner's helmet in mitigating ground fall-related head and neck injuries should be critically analyzed.

Keywords. Ground fall; biomechanical analysis; head; neck; helmet; miner safety.

1. Introduction

Ground movements (roof, rib, rock falls) pose a significant challenge to the miner's safety [1]. While the casualties during mining operations have reduced, significant numbers of miners continue to die [1]. Over the past decade, the mining industry has been forced to explore new terrains due to decreasing ore grades, deeper deposits, harder rock mass, and an ever-increasing need for rare-earth minerals [2–8]. This has resulted in underground mining and mining in caves, wherein operations have to be performed in complex, congested, and risky environments [4, 6, 8].

For the underground mines, the ground falls pose the highest risk of injury and fatality [8]. A recent study reports 3,532, 519, 177, and 85 coal mine-related fatalities in China, India, USA, and South Africa, respectively, between 2006 and 2010 [9]. The majority of these fatalities are either due to ground falls or explosions [9]. In these challenging times for the mining sector, the mine workers are at continuous risk from mine-related fatalities [9–12]. Directorate General of Mines Safety, Government of India [13] has reported 95 deaths, 82 fatal injuries, and 226 severe injuries due to ground falls from 2010 to 2015. These data suggest that the miner's safety due to ground falls is a serious, life-threatening health concern, especially in the era of underground mining, which includes mining at depths as large as 500 feet. This imposes a socioeconomic, legal, and moral burden on the mining sector. Head and neck are typically injured organs in fatal and severe injuries [1, 9, 13, 14]. The effectiveness of current helmets in protection against ground falls is not known [13].

Surprisingly, to the best of the authors' knowledge, direct work on understanding ground fall-related mine fatalities is not available in the literature. A few investigations (e.g., see [15, 16]) study the effect of a mine explosion on occupant safety in a seated vehicle. The goal of this work is to investigate the head-neck responses under simulated roof falls. We also evaluate the efficacy of helmets for protection against roof falls. Towards this end, a simplified, full-body human finite element (FE) model was built. We study the effect of helmet material, helmet layer configuration, and roof

Supplementary Information The online version contains supplementary material available at https://doi.org/10.1007/s12046-022-02028-5.

*For correspondence
Published online: 03 December 2022

velocity on the resulting biomechanical response. The biomechanical response is evaluated in terms of maximum principal strain and von Mises stress in the brain and resultant reaction force and reaction moment at the neck bottom.

The manuscript is organized as follows. In the methods section, we describe details of the full-body human FE model, loading and boundary conditions, and solution scheme. In the results section, we present a comparison of FE simulation and experimental results for model validation. This is followed by the detailed biomechanical analysis of head-neck response with and without the helmet. In the next section of the discussion, we discuss the important insights from this work and compare them with the relevant literature. The key findings are summarized in the conclusion section.

2. Methods

2.1 *Finite element (FE) human model*

A simplified, full-body, FE human model (figure 1) with a mass of 78.6 kg and height of 174.9 cm [17] in a standing position is built. The model consists of a simplified spherical head surrogate (comprising skull and brain), neck, and lower body. The inner diameter and the thickness of the skull are 150 mm and 10 mm, respectively. The inner diameter and thickness of the skull are selected based on the dimensions of the human skull [17–19]. For the spherical head, we obtain a head mass of 3.22 kg, which is close to the mass of the human head ($\sim$4.5 kg) of an average adult male [19]. Even though the inner diameter and the thickness of the skull are selected based on the dimensions of the human skull [17–19], the differences in the mass between the spherical head and the anatomically accurate human head arise from other geometric differences between spherical head and CT and MRI based head model. Note that, in this work, we have used a spherical head for (a) simplicity and (b) as experimental data on brain deformation, generated in-house, was available for the spherical head. This experimental data is used for model validation. The geometry, dimensions, and materials of the neck are based on the Hybrid-III neck [20]. A flexion angle of 25° is provided to the neck (figure 1) as the naturally positioned cervical spine has a flexion angle of $\sim$25° [21]. The roof is modeled as a cuboid of 450 mm$\times$350 mm$\times$100

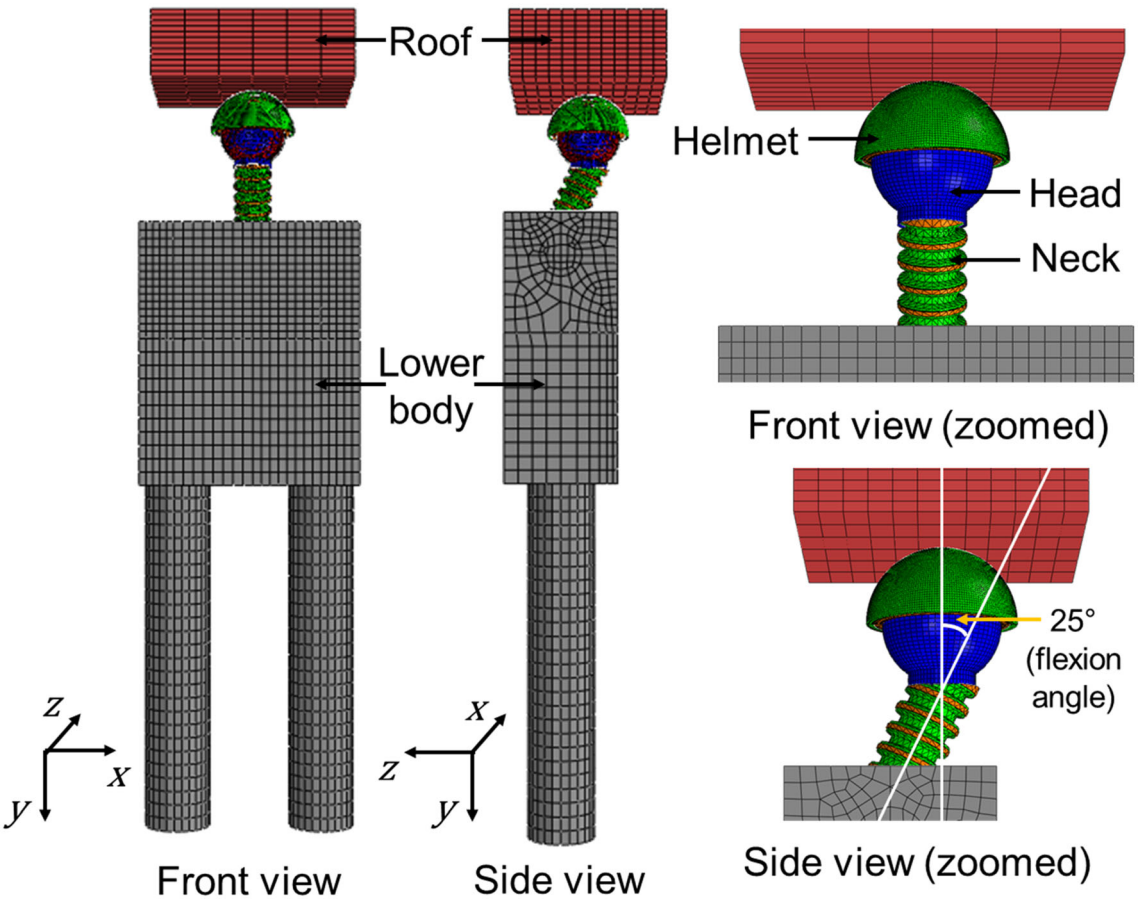

Figure 1. A simplified, full-body human finite element (FE) model.

mm. Roof mass of 50 kg is considered. The helmet is modeled as a hemispherical structure with a thickness of 10 mm for each layer. Five different helmet configurations are considered. The three types of existing double-layered helmets, helmets I-III (table 1), are selected from the literature [18, 22–24]. Triple-layered helmet IV with additional Extruded Polystyrene (XPS) layer on the top of hard Acrylonitrile butadiene styrene (ABS) layer is also considered. Hypothetical helmet V made up of only XPS is also considered (table 1).

Brain is modeled as a hyperelastic solid using neo-Hookean strain energy function, which has the following form.

$$U = C_{10}\left(\overline{\lambda}_1^2 + \overline{\lambda}_2^2 + \overline{\lambda}_3^2 - 3\right) + \frac{1}{D_1}(J-1)^2 \qquad (1)$$

where, $C_{10} = \frac{\mu_0}{2}$ and $D_1 = \frac{2}{K_0}$ are the material parameters, and $\overline{\lambda}_i = \frac{\lambda_i}{\sqrt[3]{J}}$ are the deviatoric principal stretches. J and λ_i are the Jacobian and principal stretches, respectively. Time dependent behavior of brain simulant is modeled using a quasilinear viscoelastic function [25], expressed as

$$\mu(t) = \mu_0 \times \left[1 - \sum_{i=1}^{N} g_i(1 - e^{-t/\tau_i})\right] \qquad (2)$$

where, μ_0 is the instantaneous shear modulus and g_i, and τ_i are the material constants.

The foam pads (Helmet-I) are modeled as a linear, viscoelastic material. The properties of foam pads are taken from Moss *et al.* [26], who obtained the properties from low-rate compression and acoustic testing. All other structures are modeled as linear, elastic material with properties (table 1) adopted from the literature [18, 19, 22]. Note that the rate-dependent properties are not available for these structures. Hence, we relied on linear, elastic material properties; consistent with the literature [19, 27–30]. The model is discretized to yield 5,883, 13,500, 13,326 hexahedral elements on the skull, brain, and lower body,

Table 1. Material properties used in the FE model (a) elastic properties (b) viscoelastic properties.

Substructure	Density (kg/m^3)	Mass (kg)	Elastic modulus (MPa)	Poisson's ratio
(a)				
Skull	1710	1.38	5370	0.19
Brain	1040	1.84	–	0.49
Hybrid-III Neck		1.67		
Aluminium	3200		70000	0.36
Rubber	2500		4	0.49
Body	1040	75.38	2200	0.32
Roof (Concrete)	2300	50	14000	0.2
Helmet I		0.682		
Kevlar	1230		6000	0.33
Foam Pads	136			0.49
Helmet II		0.622		
Acrylonitrile butadiene styrene (ABS)	1200		2000	0.37
Extruded Polystyrene (XPS)	26		17.7	0.35
Helmet III		0.626		
Polycarbonate	1210		2200	0.37
Expanded PolyStyrene (EPS)	22		18	0.05
Helmet IV		0.638		
Extruded Polystyrene (XPS)	26		17.7	0.35
Acrylonitrile butadiene styrene (ABS)	1200		2000	0.37
Extruded Polystyrene (XPS)	26		17.7	0.35
Helmet V		0.024		
Extruded Polystyrene (XPS)	26		17.7	0.35
Extruded Polystyrene (XPS)	26		17.7	0.35

Substructure	
(b)	
Brain	neo-Hookean hyperelastic: $\mu_0 = 2588$Pa, $\mu_\infty = 1717Pa$, $g_1 = 0.17, g_2 = 0.17$, $\tau_1 = 0.0021sec, \tau_2 = 0.03sec$
Foam Pads	$\mu_0 = 2000k$Pa, $\mu_\infty = 20.1kPa, g = 0.98995$ $\tau = 0.01sec$

respectively, and 13,243 tetrahedral elements on the neck. The interfaces between various structures of the body are considered 'tied' (i.e., no sliding, no separation), whereas the interface between the head and the helmet is treated as frictionless sliding.

2.2 *Loading and boundary conditions*

The roof has been given an initial velocity at time t = 0. The human model is subjected to dynamic loading as the impact is established between the roof and the human model. The baseline case of roof mass 50 kg, roof velocity 3 m/s oriented at $+15^0$ with neck axis is considered (figure 2a). This angle is considered based on Nightingale *et al.* [21], who found that the highest risk for injury occurs within ±30° of the axis of the neck (cervical spine). The effect of roof velocity on the biomechanical response has been studied by changing the initial roof velocity. The kinematic coupling is used to couple all the nodes at the neck bottom to a single reference node located in the center of the neck bottom (figure 2b). In order to calculate reaction forces and reaction moments, the reference node is constrained in all degrees of freedom. We have also studied the response with the unconstrained neck. The responses between constrained and unconstrained neck are similar (Supplementary Fig. 1). Further, lower body displacements (Supplementary Fig. 2) are negligible (< 1 mm) as compared to the head-neck displacements (> 5 mm).

2.3 *Solution scheme*

FE model is solved using a nonlinear, transient, dynamic procedure using an explicit scheme (Abaqus, Dassault Systemes Simulia Corp). The total simulated time of 5 ms is considered. A typical run requires ∼180 minutes of CPU time using an Intel i7-8550U processor (4 cores, processor speed 1.8 GHz, 7.84 GB memory).

3. Results

3.1 *Model validation*

The head and neck models are validated against the experimental data in the literature and data generated in-house. Myers and Nightingale [31] measured resultant neck force in post-mortem human subjects for a range of normal and oblique impacts using a vertical drop setup impacting a rigid surface. Using a linear impactor system, we have measured 2D strains in a brain simulant in a hemispherical head (skull-brain) model subjected to impact loading. The complete details of the experiment are available in Singh *et al.* [32].

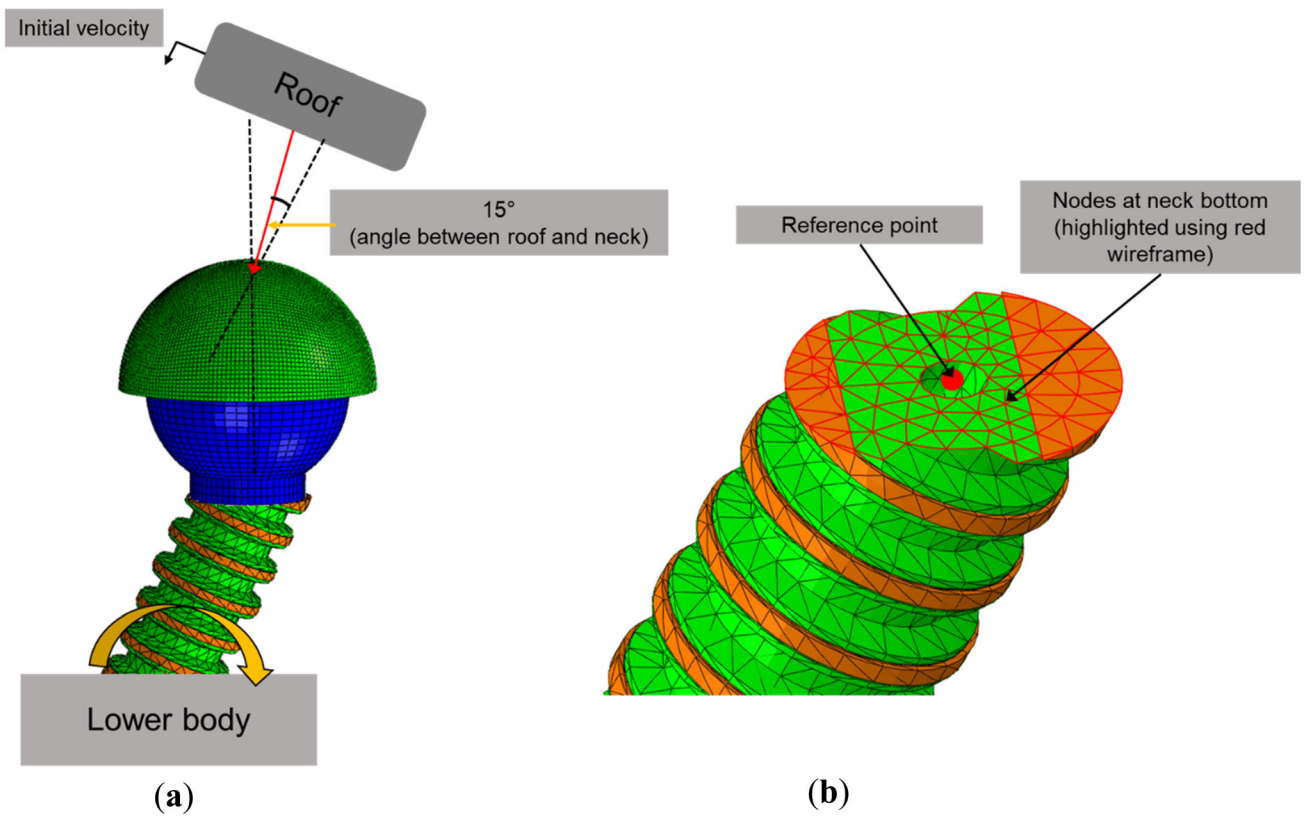

Figure 2. (**a**) Loading and (**b**) boundary conditions.

Briefly, the hemispherical head (skull-brain) was mounted on the Hybrid-III neck (Humanetics, Farmington Hills, MI) and subjected to impact loading using a linear impactor system. The motion of the brain simulant to impact loading was captured using a high-speed camera (Phantom v341, Vision Research, Inc., Wayne, NJ). A midsagittal plane (open surface) was selected for imaging, and a frame rate of 2500 frames/s was used. To capture the motion of the midsagittal plane and quantify strains, a random speckles pattern was applied on the brain simulant. Imaging was done at spatial and temporal resolutions of 0.38 mm/pixel and 0.4 ms, respectively. 2D strains in a brain simulant were calculated from acquired images using a digital image correlation technique [33].

Digital image correlation uses subset based image registration algorithms to track the relative displacements of material points between a reference image and a current image. The displacements of a subset are obtained by maximizing a correlation function between the reference image and the deformed image. 2D, Green-Lagrangian strains are calculated from displacements using pointwise least square fit on a subset. Large deformations are accounted for by updating the boundary of the region of interest based on the displacement field. Additional details regarding the estimation of brain strains using digital image correlation are available in Singh *et al.* [32] and hence avoided here.

The aforementioned experiments are simulated using a computational human model used in this work, and the model response is compared against corresponding experimental data. The agreement between simulations and experiments is reasonable in terms of resultant neck force (table 2), spatiotemporal evolution of brain strain (figure 3, table 3a), and the peak values of brain strain (table 3b).

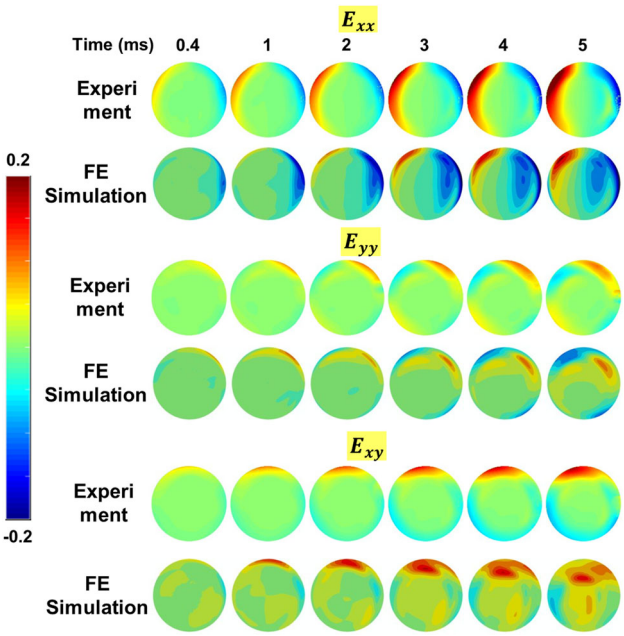

Figure 3. Comparison of 2D brain strains between the experiment and simulation for a hemispherical head model consisting of skull and brain for an impact velocity of 1 m/s.

4. Head-neck biomechanical response with and without the helmet

The biomechanical response is evaluated in terms of maximum principal strain and von Mises stress in the brain and resultant reaction force and reaction moment at the neck bottom. We have focused on early time response ($\sim$5 ms), which is relevant for moderate and severe injuries [31, 34]. It has been demonstrated that the dynamics in moderate and severe neck injuries play out within a few milliseconds [31, 34].

Figure 4 shows the biomechanical response of the brain and neck for the baseline case (roof velocity 3 m/s), with and without the helmet (helmet II). For the brain, the response is shown for an element just beneath the impact location (i.e., coup site), where the mechanical field values are maximum. The helmet reduces the peak maximum principal strain and peak von Mises stress in the brain by 34 % and 47 %, respectively. On the contrary, the use of the helmet increases the magnitude of peak neck reaction force and peak neck reaction moment by 68 % and 86 %, respectively. This increase in neck force and neck moment is due to the increase in mass of the system due to the addition of the helmet.

Table 2. Comparison of peak resultant neck force between the simulation and experiment (Myers and Nightingale).

Velocity (m/s)	Angle of impact (^{o} degrees)	Peak resultant neck force (N)		% error
		simulation	experiment	
3.18	$+15^o$	3058	2612	17.07
3.26	$+15^o$	1784	1895	5.86
3.2	0^o	1810	1973	8.26

Table 3. (a) Metrics of agreement of strain fields between experiment and simulation for an impact velocity of 1 m/s. (b) Comparison of peak brain strains between the simulation and experiment for an impact velocity of 1 m/s.

Time[1] (ms)	Strain	Index of agreement[2], d_r	Coefficient of efficiency[2], E_2	Root mean square error-standard deviation ratio[2], RSR	Correlation scores[3], CS
(a)					
3	E_{xx}	0.86	0.75	0.60 (good[3])	92.50 (excellent[3])
	E_{yy}	0.88	0.76	0.59 (good[3])	93.30 (excellent[3])
	E_{xy}	0.89	0.78	0.56 (good[3])	94.90 (excellent[3])

Strain	Peak Strain		% error
	Simulation	Experiment	
(b)			
E_{xx}	0.19	0.20	5
E_{yy}	0.15	0.16	6.25
E_{xy}	0.20	0.19	5.26

[1] Values at a representative time point of 3 ms are shown. A similar agreement is obtained at other time points.

[2] Details regarding these quantitative measures are available in Ganpule *et al.* [27]

[3] Qualitative performance ratings are available in [27, 55]

4.1 *Effect of helmet material and layer configuration on biomechanical response*

As stated earlier, three types of existing double-layered helmets (table 1) are selected from the literature [18, 22–24]. A triple-layered helmet IV with an additional XPS layer on top of the hard ABS layer is also considered. Hypothetical helmet V made up of only XPS is also considered (table 1). The biomechanical responses at the brain and neck (figure 5) are estimated with each helmet for the baseline case (roof velocity 3 m/s). Compared to the helmet I, the peak values of maximum principal strain, von Mises stress, neck force, and neck moment are reduced by $\sim$20 %, $\sim$20 %, $\sim$2 %, and $\sim$10 %, respectively, in helmets II-IV. This is due to the differences in the mass and impedance (i.e., ρc) properties between the helmet I and helmets II-IV. Helmets II-IV show equivalent peak values for the aforementioned biomechanical variables. With respect to helmet I, the occurrence of peak (i.e., time at which peak occurs) is delayed for helmets II, III due to the lower impedance of helmets II, III. The occurrence of the peak is further delayed for helmet IV due to the additional XPS layer. For the hypothetical helmet V, peak values of biomechanical variables are reduced, and the occurrence of the peak is further delayed as compared to all other helmet configurations due to the smaller mass of the helmet and reduced impedance. Specifically, compared to helmet I, the peak values of maximum principal strain, von Mises stress, neck force, and neck moment are reduced by 24%, 20%, 37%, and 45%, respectively, in helmet V. However, note that, for helmet V, neck force and neck moment are yet marginally increased by 6.44 % and 2.38 %, respectively, compared to the no helmet case.

4.2 *Sensitivity of biomechanical response to roof velocity*

Figure 6 shows the biomechanical response for three different roof velocities 1 m/s, 3 m/s, and 5 m/s. The results are sensitive to the roof velocity; peak values of biomechanical parameters increase with an increase in roof velocity.

5. Discussion

Mine-related fatalities constitute a significant health concern in the age of underground mining and mining in caves, wherein operations have to be performed in complex, congested, and risky environments [2–8]. Lack of awareness and poor quality of life has resulted in these fatalities going unnoticed or forgotten without any significant protocol or policy changes [9–12]. Roof and ground falls account for a significant portion of mine fatalities during underground mining and mining in caves [8], with head and neck injuries being most common [1, 9, 13, 14]. The biomechanical response of a miner against ground falls is not known. Further, to the best of the authors' knowledge, the role of the miner's helmet in

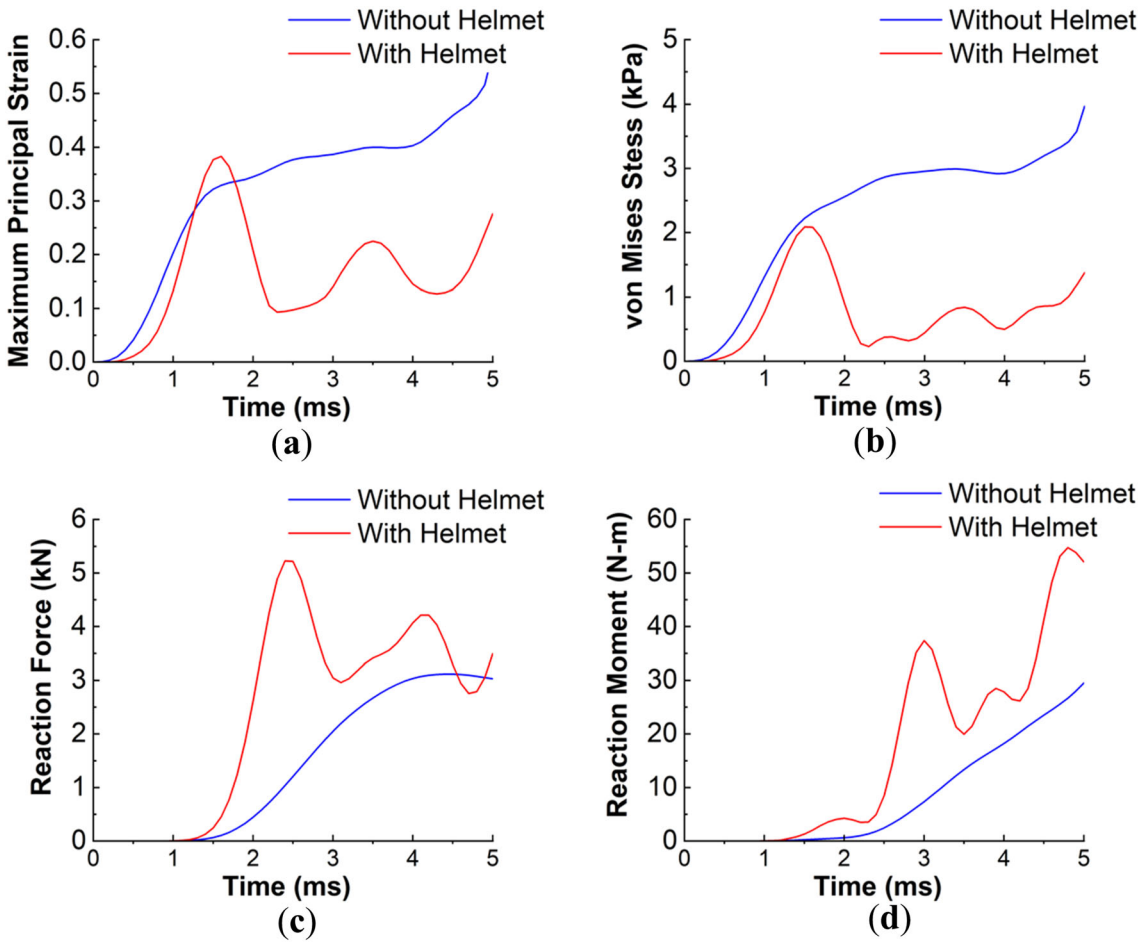

Figure 4. Biomechanical response of the brain and neck with and without the helmet for the baseline case (roof velocity 3 m/s). (**a**) maximum principal strain (**b**) von Mises stress in the brain (**c**) resultant neck reaction force (**d**) resultant neck reaction moment.

mitigating ground fall-related injuries has never been evaluated.

Using a simplified full-body human model, we have studied the head-neck biomechanical response of human against a roof fall. The model has been validated against relevant, available experimental data. The agreement of brain strains and neck reaction forces between experiments and simulation is reasonable (figure 3, tables 2 and 3). Nightingale *et al.* [21] measured neck reaction forces in post-mortem human subjects for an impactor velocity of 3.14 $\pm$ 0.19 m/sec for a range of normal and oblique impacts using a vertical drop setup. Camacho *et al.* [35] have conducted computational simulations using a finite element based head-neck model. These studies report peak neck force and peak neck moment in the range of 2-4 kN and 20-80 N-m, respectively. For no helmet case, we obtain peak neck force and peak neck moment of 3 kN and 25 N-m, respectively. For the helmet case, we obtain peak neck force and peak neck moment of 5 kN and 55 N-m, respectively. The peak values of neck force and neck moment are consistent with the aforementioned studies of Nightingale *et al.* [21] and Camacho *et al.* [35]. Further, for the simulated time considered in this work, the shape of the neck force and neck moment time histories are consistent with the ones observed in Nightingale *et al.* [21].

In response to a roof fall, the head and neck undergo compression. Since the brain does not follow the motion of the skull, it induces significant strains and stresses in the brain. As compared to the no-helmet case, the addition of the helmet reduces the peak maximum principal strain and peak von Mises stress in the brain by up to $\sim$47 % and 59%, respectively. However, the helmet increases the peak resultant neck reaction force and peak resultant neck reaction moment by up to $\sim$68 % and 86 %, respectively. This is due to the increase in the mass of the system due to the addition of the helmet. This trend remains similar for all helmet configurations except for the hypothetical helmet V made up of only XPS, for which peak neck response is similar (equivalent) to the no helmet case. Adding the softer layer on top of the hard layer (helmet IV) did not reduce the peak biomechanical response. The softer layer on top of the hard layer only delayed the occurrence (i.e., time) of the peak values.

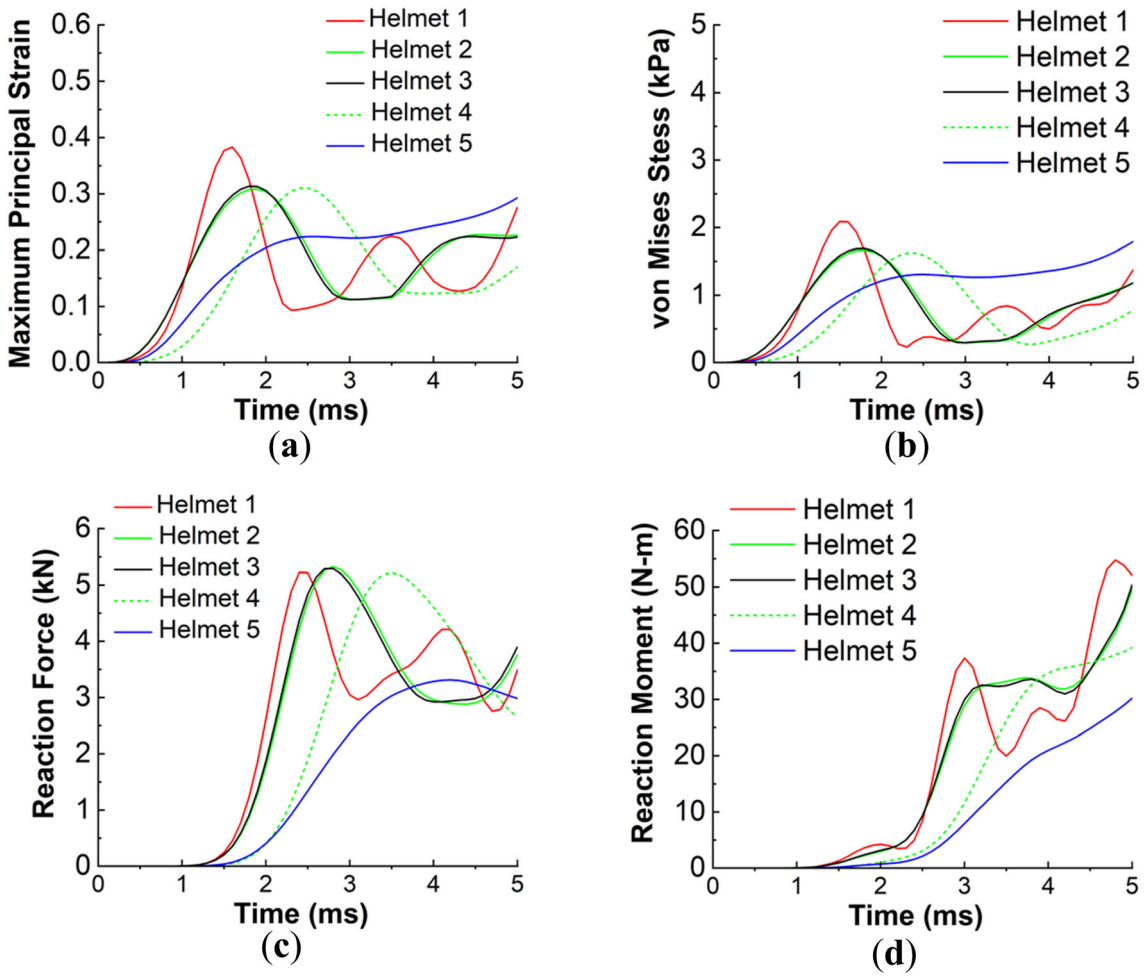

Figure 5. Biomechanical response of the brain and neck for various helmet configurations for the baseline case (roof velocity 3 m/s). (**a**) maximum principal strain (**b**) von Mises stress in the brain (**c**) resultant neck reaction force (**d**) resultant neck reaction moment.

We also performed additional simulations by incorporating a nonlinear stress-strain response for EPS [36]. Results did not alter significantly with the incorporation of nonlinear stress-strain response. In our simulations, the peak strains in XPS and EPS helmet layers are $\sim$10%. Densification and nonlinearity in EPS are observed at much higher strains ($\sim$60 %) [36]. Thus, the energy absorption regime of these materials is not utilized for the type of strains seen in our simulations. Future target helmet materials should focus on materials with densification at smaller strains or shape memory alloys (e.g., see [37] and references therein) capable of attenuating the incoming load at smaller strains and within shorter timescales implied in impact or blast.

These observations, yet non-intuitive, are not fully surprising. Jadischke *et al.* [38] conducted pendulum impact tests on Hybrid III head and neck with different helmet configurations. They found that the addition of the helmet reduced the peak head accelerations by up to 44% and increased the peak resultant neck forces by up to 49%. They attributed the increase in neck forces to the increase in mass of the system due to the addition of the helmet. They concluded that the increased neck forces enhance the risk of concussion. Collins *et al.* [39] measured neck strength in high school athletes at the beginning of the sports season. They monitored reported concussion incidence and athletic exposure data during the course of a sports season. They found that neck strength was a significant predictor of concussion in high school athletes.

Most of the retrospective investigations studying motorbike accidents suggest that motorbike helmets are protective to prevent head and brain injuries. On the contrary, the role of motorbike helmets in reducing neck injuries is controversial and a topic of intense discussion and scrutiny [40]. Several retrospective studies suggest that helmets increase the risk of neck injuries [41–45], while a few other retrospective studies suggest that helmets do not increase the risk of neck injury during motorbike accidents [40, 46–49] as compared to the no helmet scenario. To the best of the authors' knowledge, biomechanical and retrospective investigations into the miner's helmet are not available, and this work is one of the first of such studies.

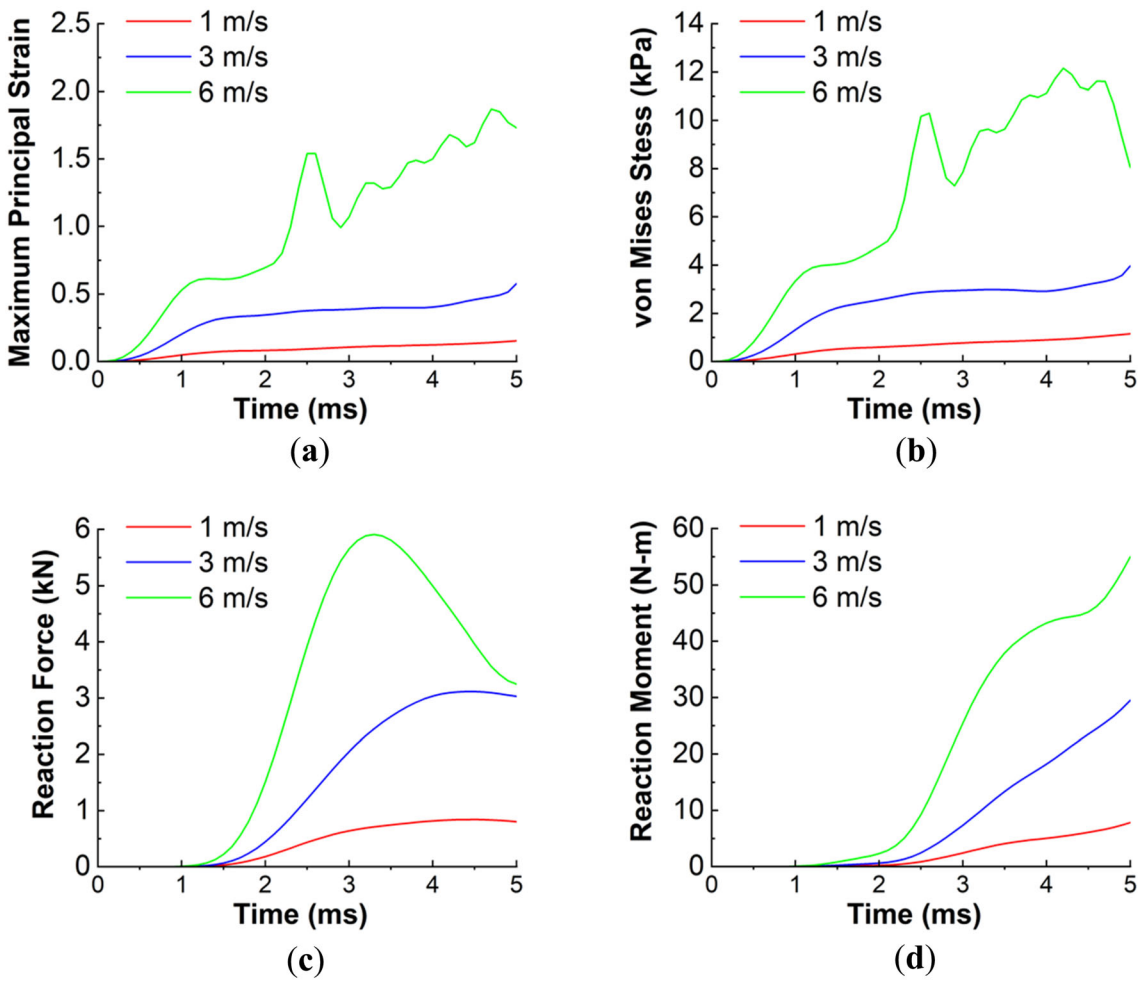

Figure 6. Effect of roof velocity on biomechanical response. (**a**) maximum principal strain (**b**) von Mises stress in the brain (**c**) resultant neck reaction force (**d**) resultant neck reaction moment.

Our biomechanical analysis suggests that the neck loads are increased due to the use of helmets. Thus, other alternatives such as the use of a neck collar (e.g., see [50–52]) during mining operations should be explored. Extrapolating our results to the risk of injury is not considered, as a simplified model is used in this work. We emphasize caution while extrapolating our results to the risk of injury with and without the use of the helmet. Our results, however, underscore the fact that the relationship between the helmet and neck load should be carefully considered in future biomechanical studies and helmet designs. Further, the protection offered by the helmets in preventing brain injury should also be critically evaluated as maximum principal strain values predicted by a simplified head model are above reported critical injury threshold values [28, 53] for roof velocities of 3 m/s and 6 m/s. The von Mises stress value predicated by simplified head model for a roof velocity of 6 m/s is above reported critical threshold value for 50% probability of sustaining a mild traumatic brain injury [54].

This work has several limitations. A simplified human model (including simplified head-neck model) is considered in this work. Even though the model has been validated for brain and neck responses, the absolute values obtained using this model should be considered in a simplified modeling context. Nonetheless, the model captures overall trends with and without helmets that are consistent with the literature.

6. Conclusions

Biomechanical response of human head and neck under a roof fall has been studied using a simplified FE model. The model response has been compared against relevant, available experimental data. Various helmet configurations have been studied. Some of the key findings of this work are:

- Helmets are effective in reducing the strains and stresses in the brain. As compared to the no-helmet case, the addition of the helmet reduces the peak maximum principal strain and peak von Mises stress in the brain by up to $\sim$47 % and 59%, respectively.

- Helmets increase the peak neck reaction forces and peak neck reaction moments. As compared to the no-helmet case, the addition of helmet increases peak resultant neck reaction force by up to $\sim$68 % and peak resultant neck reaction moment by up to 86 %, respectively.
- Helmet layer configuration affects the biomechanical response in terms of the timing of the peak values and their magnitudes. However, the overall trends remain unchanged by helmet layer configuration. Mass and impedance of the helmet layers play a critical role in dictating the magnitude and timing of peak values.
- The neck responses between the hypothetical helmet made of softer layers only and no helmet case are equivalent. Hence, alternative strategies should be considered to reduce the neck load.
- Peak values of biomechanical parameters increase with the increase in roof velocity.

These results provide preliminary (but unique and novel) insights into the biomechanical response of head and neck under the roof fall, with implications in designing the next generation of the miner's helmet, especially to cater to the needs of the underground mining sector.

Acknowledgments

SG acknowledges financial support from the Department of Science and Technology (DST) under the Grant ECR-2017-000417.

Declarations

Conflict of interest The authors declare that they have no conflict of interest.

References

[1] Pappas D and Mark C 2012 Roof and rib fall incident trends: a 10-year profile. *Trans. Soc. Min. Metall. Explor.* 330: 462–478

[2] Haque N, Hughes A, Lim S and Vernon C 2014 Rare earth elements: overview of mining, mineralogy, uses, sustainability and environmental impact. *Resources* 3(4): 614–635

[3] Huang X, Zhang G, Pan A, Chen F and Zheng C 2016 Protecting the environment and public health from rare earth mining. *Earth's Future* 4(11): 532–535

[4] Zhang L 2014 Towards sustainable rare earth mining: a study of occupational & community health issues. University of British Columbia

[5] Holland M 2020 Reducing the health risks of the copper, rare earth and cobalt industries: Transition to a circular low-carbon economy

[6] Froude M J and Petley D N 2018 Global fatal landslide occurrence from 2004 to 2016. *Nat. Hazards Earth Syst. Sci.* 18(8): 2161–2181

[7] Kohler J L 2015 Looking ahead to significant improvements in mining safety and health through innovative research and effective diffusion into the industry. *Int. J. Min. Sci. Technol.* 25(3): 325–332

[8] Pokhrel L R and Dubey B 2013 Global scenarios of metal mining, environmental repercussions, public policies, and sustainability: a review. *Crit. Rev. Environ. Sci. Technol.* 43(21): 2352–2388

[9] Harris J, Kirsch P, Shi M, Li J, Gagrani A, Krishna E, Tabish A, Arora D, Kothandaraman K and Cliff D 2014 Comparative analysis of coal fatalities in Australia, South Africa, India, China and USA, 2006–2010. In: *Proceedings of the 2014 Coal Operators' Conference*, University of Wollongong

[10] Rehman A U, Emad M Z, Khan M U, Saleem M A and Saki S A 2021 Investigation and analysis of fatal accidents reporting practices in the Punjab province of Pakistan and remedial measures. *Resour. Policy* 73: 102186

[11] Farrenkopf M 2019 Accidents and mining: The problem of the risk of explosion in industrial coal mining in global perspective. In: *Making Sense of Mining History*, Routledge, pp. 193-211

[12] Zhang J, Fu J, Hao H, Fu G, Nie F and Zhang W 2020 Root causes of coal mine accidents: Characteristics of safety culture deficiencies based on accident statistics. *Process Saf. Environ. Prot.* 136: 78–91

[13] Directorate general of mines safety-Ministry of Labour & Employment-Government of India 2015 Statistics of mines in India Volume-I (Coal). New Delhi, India

[14] West Virginia Office of Miners' Health-Safety and Training, 2017, Report of fatal Investigation: Roof fall. Charleston, WV

[15] Lee K 1998 Biomechanical Response of the Human Body Inside a Military Vehicle Exposed to Mine Explosion. Naval Postgraduate School, Monterey CA

[16] Nilakantan G and Tabiei A 2009 Computational assessment of occupant injury caused by mine blasts underneath infantry vehicles. *Int. J. Veh. Struct. Syst.* 1(1–3): 50

[17] Gayzik F S, Moreno D P, Geer C P, Wuertzer S D, Martin R S and Stitzel J D 2011 Development of a full body CAD dataset for computational modeling: a multi-modality approach. *Ann. Biomed. Eng.* 39(10): 2568–2583

[18] Ganpule S, Gu L, Alai A and Chandra N 2012 Role of helmet in the mechanics of shock wave propagation under blast loading conditions. *Comput. Methods Biomech. Biomed. Eng.* 15(11): 1233–1244

[19] Mao H, Zhang L, Jiang B, Genthikatti V V, Jin X, Zhu F, Makwana R, Gill A, Jandir G and Singh A 2013 Development of a finite element human head model partially validated with thirty five experimental cases. *J. Biomech. Eng.* 135(11): 111002

[20] Foster J K, Kortge J O and Wolanin M J 1977 Hybrid III—a biomechanically-based crash test dummy. *SAE Trans.* 86: 3268–3283

[21] Nightingale R W, McElhaney J H, Camacho D L, Kleinberger M, Winkelstein B A and Myers B S 1997 The dynamic responses of the cervical spine: buckling, end conditions, and tolerance in compressive impacts. *SAE Trans.* 106: 3968–3988

[22] Gholampour S, Hajirayat K, Erfanian A, Zali A R and Shakouri E 2017 Investigating the role of helmet layers in reducing the stress applied during head injury using FEM. *Int. Clin. Neurosci. J.* 4(1): 4–11

[23] http://www.safety-helmet.com/safetyhelmet/mining-helmet.html. Accessed September 2021
[24] http://www.concordhelmet.com/mining-industrial-helmets.html. Accessed September 2021
[25] Fung Y-C 2013 Biomechanics: Mechanical Properties of Living Tissues. Springer Science & Business Media, New York
[26] Moss W C, King M J and Blackman E G 2009 Skull flexure from blast waves: a mechanism for brain injury with implications for helmet design. *Phys. Rev. Lett.* 103(10): 108702
[27] Ganpule S, Daphalapurkar N P, Ramesh K T, Knutsen A K, Pham D L, Bayly P V and Prince J L 2017 A three-dimensional computational human head model that captures live human brain dynamics. *J. Neurotrauma* 34(13): 2154–2166
[28] Giordano C and Kleiven S 2014 Evaluation of axonal strain as a predictor for mild traumatic brain injuries using finite element modeling. *Stapp Car Crash J.* 58: 29
[29] Ji S, Zhao W, Ford J C, Beckwith J G, Bolander R P, Greenwald R M, Flashman L A, Paulsen K D and McAllister T W 2015 Group-wise evaluation and comparison of white matter fiber strain and maximum principal strain in sports-related concussion. *J. Neurotrauma* 32(7): 441–454
[30] Schwartz D, Guleyupoglu B, Koya B, Stitzel J D and Gayzik F S 2015 Development of a computationally efficient full human body finite element model. *Traffic Inj Prev.* 16(sup1): S49–S56
[31] Myers B S and Nightingale R W The dynamics of head and neck impact. In: *Proceedings of the 1997 international IRCOBI conference on the biomechanics of* impact, Hanover
[32] Singh A, Ganpule S G, Khan M K and Iqbal M A 2021 Measurement of brain simulant strains in head surrogate under impact loading. *Biomech. Model. Mechanobiol.* 20(6): 2319–2334
[33] Blaber J, Adair B and Antoniou A 2015 Ncorr: open-source 2D digital image correlation matlab software. *Exp. Mech.* 55(6): 1105–1122
[34] Nightingale R W, McElhaney J H, Richardson W J and Myers B S 1996 Dynamic responses of the head and cervical spine to axial impact loading. *J. Biomech.* 29(3): 307–318
[35] Camacho D L, Nightingale R W and Myers B S 2001 The influence of surface padding properties on head and neck injury risk. *J. Biomech. Eng.* 123(5): 432–439
[36] Chen W, Hao H, Hughes D, Shi Y, Cui J and Li Z-X 2015 Static and dynamic mechanical properties of expanded polystyrene. *Mater. Design* 69: 170–180
[37] Pant D C and Pal S 2019 Phase transformation and energy dissipation of porous shape memory alloy structure under blast loading. *Mech. Mater.* 132: 31–46
[38] Jadischke R, Viano D C, McCarthy J and King A I 2016 The effects of helmet weight on hybrid III head and neck responses by comparing unhelmeted and helmeted impacts. *J. Biomech. Eng.*, 138(10): 101008
[39] Collins C L, Fletcher E N, Fields S K, Kluchurosky L, Rohrkemper M K, Comstock R D and Cantu R C 2014 Neck strength: a protective factor reducing risk for concussion in high school sports. *J. Prim. Prev.* 35(5): 309–319
[40] Liu B C, Ivers R, Norton R, Boufous S, Blows S and Lo S K 2008 Helmets for preventing injury in motorcycle riders. *Cochrane Database Syst. Rev.* (1)
[41] Peter K and Krantz G 1985 Head and neck injuries to motorcycle and moped riders—with special regard to the effect of protective helmets. *Injury* 16(4): 253–258
[42] Uhrenholt L, Thomsen C K, Hansen K, Boel L W T and Freeman M D 2020 Relationship between head and neck injuries and helmet use in fatal motorcycle and moped crashes in Denmark. *Scand. J. Forensic Sci.* 26(1): 1–7
[43] Kasantikul V, Ouellet J V and Smith T 2003 Head and neck injuries in fatal motorcycle collisions as determined by detailed autopsy. *Traffic Inj. Prev.* 4(3): 255–262
[44] Goldstein J P 1986 The effect of motorcycle helmet use on the probability of fatality and the severity of head and neck injuries: a latent variable framework. *Eval. Rev.* 10(3): 355–375
[45] Ooi S, Wong S, Yeap J and Umar R 2011 Relationship between cervical spine injury and helmet use in motorcycle road crashes. *Asia Pac. J. Public Health* 23(4): 608–619
[46] Lam C, Wiratama B S, Chang W-H, Chen P-L, Chiu W-T, Saleh W and Pai C-W 2020 Effect of motorcycle helmet types on head injuries: evidence from eight level-I trauma centres in Taiwan. *BMC Public Health* 20(1): 1–11
[47] Sarkar S, Peek C and Kraus J F 1995 Fatal injuries in motorcycle riders according to helmet use. *J. Trauma Acute Care Surg.* 38(2): 242–245
[48] Khor D, Inaba K, Aiolfi A, Delapena S, Benjamin E, Matsushima K, Strumwasser A M and Demetriades D 2017 The impact of helmet use on outcomes after a motorcycle crash. *Injury* 48(5): 1093–1097
[49] Rice T M, Troszak L, Ouellet J V, Erhardt T, Smith G S and Tsai B-W 2016 Motorcycle helmet use and the risk of head, neck, and fatal injury: Revisiting the Hurt Study. *Accident Anal. Prev.* 91: 200–207
[50] Yuan W, Diekfuss J A, Barber Foss K D, Dudley J, Leach J, Narad M E, DiCesare C A, Bonnette S, Epstein J and Logan K 2021 High school sports-related concussion and the effect of a jugular vein compression collar: a prospective longitudinal investigation of neuroimaging and neurofunctional outcomes. *J. Neurotrauma(ja)* 38: 2811–2821
[51] Mannix R, Morriss N J, Conley G M, Meehan W P III, Nedder A, Qiu J, Float J, DiCesare C A and Myer G D 2020 Internal jugular vein compression collar mitigates histopathological alterations after closed head rotational head impact in swine: A pilot study. *Neuroscience* 437: 132–144
[52] Yuan W, Leach J, Maloney T, Altaye M, Smith D, Gubanich P J, Barber Foss K D, Thomas S, DiCesare C A and Kiefer A W 2017 Neck collar with mild jugular vein compression ameliorates brain activation changes during a working memory task after a season of high school football. *J. Neurotrauma* 34(16): 2432–2444
[53] Bain A C and Meaney D F 2000 Tissue-level thresholds for axonal damage in an experimental model of central nervous system white matter injury. *J. Biomech. Eng.* 122(6): 615–622
[54] Zhang L, Yang K H and King A I 2004 A proposed injury threshold for mild traumatic brain injury. *J. Biomech. Eng.* 126(2): 226–236
[55] Moriasi D N, Arnold J G, Van Liew M W, Bingner R L, Harmel R D and Veith T L 2007 Model evaluation guidelines for systematic quantification of accuracy in watershed simulations. *Trans. ASABE* 50(3): 885–900